J|A|C|S
COMMUNICATIONS

Published on Web 04/09/2004

Exceptionally Small Attenuation Factors in Molecular Wires

Francesco Giacalone,[†] José L. Segura,[†] Nazario Martín,*[,†] and Dirk M. Guldi*[,‡]

Departamento de Química Orgánica, Facultad de Química, Universidad Complutense, E-28040 Madrid, Spain, and Radiation Laboratory, University of Notre Dame, Notre Dame, Indiana 46556

Received December 19, 2003; E-mail: nazmar@quim.ucm.es

The potential of molecular-sized materials for electronic and photonic applications has led to an ever increasing interest in developing and probing molecular-scale wires.[1] π-Conjugated oligomers, such as oligo (*p*-phenylenevinylenes) (oligo-PPVs), are among those molecules which act as efficient molecular wires.[2,3] Despite this interest, only a few reports on electron transfer through the π-conjugated chains of oligo-PPVs are known.[4] In this light, the importance of energy matching between the donor and bridge components, for achieving molecular-wire behavior, has been highlighted.[5,6]

Herein, we describe a novel series of **C_{60}−wire−*ex*TTF** ensembles that incorporate oligo-PPVs as bridges that connect π-extended tetrathiafulvalenes (*ex*TTF) (electron donor) with [60]-fullerenes (electron acceptor). The conjugation length of the oligomers in the bridges has been systematically increased. Particularly important in the design of these ensembles is the coupling of the *ex*TTF moiety to the oligomeric bridge, achieving full conjugation, which optimizes the electronic coupling between the donor and acceptor. This molecular design allows for probing effects of distance and rate at which electron-transfer processes occur, as well as the molecular-wire behavior of the oligo-PPVs.

Higher molecular weight oligo-PPVs are known to be poorly soluble in organic solvents. Thus, we pursued a stepwise procedure of tail functionalization. First, we synthesized a homologous series of soluble oligomers bearing several solubilizing alkoxy chains and two formyl groups at their terminals for further chemical transformations. Next, the linkage of *ex*TTF to the different phenylenevinylene derivatives was carried out by olefination Wittig reaction of triphenylphosphonium bromide of the TTF derivative and the formyl substituted oligomers under careful stoichiometric control. In the final step, **1**−**5** were obtained by treating monoaldehydes (*ex*TTF−oligomer−CHO) with C_{60} and sarcosine (*N*-methylglycine), *N*-(3,6,9-trioxadecyl)glycine, or *N*-octylglycine to improve the solubility, in refluxing toluene or chlorobenzene for 24 h. The reaction takes place by 1,3-dipolar cycloaddition of the "in situ" generated azomethyne ylides to C_{60},[7] yielding triads **1**, **3**−**5** as highly soluble brown solids. Triad **2**, on the other hand, was prepared by using the Wittig−Horner reaction with formyl−*ex*TTF[8] (Chart 1) (see Supporting Information).

The cyclic voltammograms of **1**−**5** (*o*DCB/MeCN, 4:1; glassy carbon as working electrode; SCE as reference electrode; Pt as counter electrode; Bu_4NClO_4 0.1 M as supporting electrolyte) revealed the first four reduction steps of the fullerene core (∼ −0.70; −1.10; −1.65; −2.10 V)[9] and the reduction of the oligo-PPV moiety at around −1.9 V.[10] On the oxidation side, a two-electron quasireversible oxidation wave to form the dication of the *ex*TTF moiety was observed at ∼0.45 V.[8] In addition, a second oxidation wave is observed in the 0.80−1.72 V range, which involves the oligo-PPV fragment and is cathodically shifted with an increase in the conjugation length of the oligomer.

Chart 1. Novel Synthesized **C_{60}−wire−*ex*TTF** Triads (**1**−**5**)

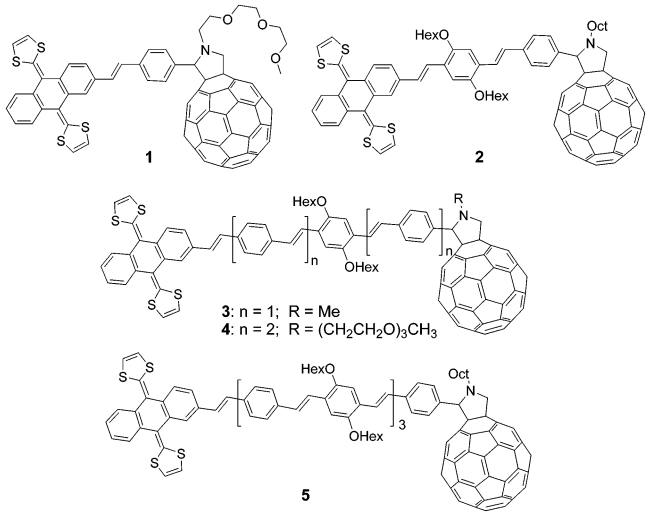

Triads **1**−**5** were probed in fluorescence and transient absorption studies. 355 nm excitation populates the singlet excited states of C_{60} (1.76 eV) and that of the oligomer (∼2.5 eV), due to overlapping absorptions. In case of exciting the oligo-PPV part, a rapid intramolecular transduction of energy funnels the excited-state energy to the fullerene core, generating ^{1}*C_{60} quantitatively. Excitation of C_{60} leads directly to ^{1}*C_{60}. Once populated, ^{1}*C_{60} powers an exothermic electron transfer ($-\Delta G_{CS}$ = ∼0.7 eV) to yield the charge-separated radical ion pairs, **$C_{60}^{\bullet-}$−wire−*ex*TTF$^{\bullet+}$**. Formation of the radical pair, **$C_{60}^{\bullet-}$−wire−*ex*TTF$^{\bullet+}$**, was followed by (i) time-resolved fluorescence (i.e., fullerene fluorescence decay at 720 nm, see Figure S2) and (ii) transient absorption (i.e., transient decay of the fullerene singlet−singlet absorption at 900 nm) spectroscopy. Spectroscopic evidence for the radical pair formation was obtained from the features, see Figure S3, developing in parallel with the disappearance of the fullerene singlet−singlet absorption. In the visible region, a 660 nm maximum corresponds to the one-electron oxidized ***ex*TTF$^{\bullet+}$**, while in the near-infrared region, the 1000 nm maximum resembles the signature of the one-electron reduced **$C_{60}^{\bullet-}$**.[11] Table S1 summarizes all of the photophysical features for **1**−**5**.

A superexchange mechanism, leading directly (see Figure S1) to **$C_{60}^{\bullet-}$−wire−*ex*TTF$^{\bullet+}$**, is imposed in **1** by the large HOMO (C_{60})−HOMO (wire) gap of 0.7 eV. In **2**−**5**, however, good electronic mixing of these two HOMOs with nearly isoenergetic levels diminishes the energy penalty for initial electron injections from the wire to ^{1}*C_{60}. Paraconjugation, which extends into the *ex*TTF donor, and the exothermic nature of the charge shift reaction are then responsible for extremely fast charge shift dynamics to form **$C_{60}^{\bullet-}$−wire−*ex*TTF$^{\bullet+}$**.

Both radical pair attributes are stable on the picosecond time scale and start to decay slowly in the nanosecond regime. Time−absorption profiles, as depicted in Figure S4, illustrate that **$C_{60}^{\bullet-}$**−

[†] Universidad Complutense.
[‡] University of Notre Dame.

10.1021/ja0318333 CCC: $27.50

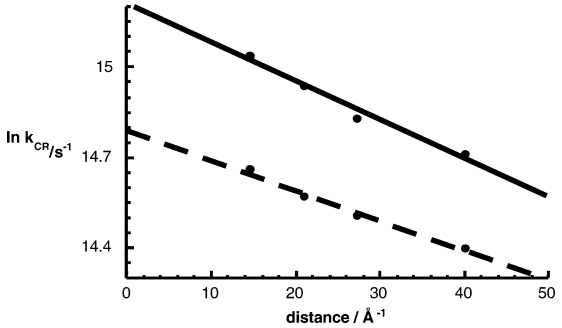

Figure 1. Distances dependence of electron-transfer rate constants in **C$_{60}$−wire−*ex*TTF** in nitrogen-saturated THF (solid line) and benzonitrile (dashed line) at room temperature.

wire−***ex*TTF**$^{\bullet+}$ decays via a single step. At room temperature, the **C$_{60}^{\bullet-}$−wire−*ex*TTF**$^{\bullet+}$ radical pair in the monomer-based ensemble (**1**) is subject to a notable stabilization, relative to the radical pair from the donor−acceptor system, in which the *ex*TTF moiety was attached directly to the pyrrolidine functionality, **C$_{60}$−*ex*TTF**. In benzonitrile, a lifetime of 204 ns was reported for this closely spaced system (R_{CC} = 9.7 Å). The monomer-based ensemble (**1**), with R_{CC} = 16.2 Å, reveals a lifetime of 430 ns. This reflects the larger separation and weaker electronic coupling. Implementation of a dimer, trimer, or pentamer oligo-PPV led to small effects on the stability of the radical pair. The first bridging unit introduces a significant barrier to electron transfer, but additional ones have only a modest effect on the barrier with the exception of **5**: 10-times longer radical pair lifetimes were noted, both in THF and in benzonitrile, which suggests smaller electronic coupling.

Plotting the charge recombination behavior as a function of donor−acceptor separation, excluding the heptameric ensemble (**5**), led to linear dependences in THF and benzonitrile. From the plots, as shown in Figure 1, we determine attenuation factors (β) as 0.01 ± 0.005 Å^{-1}, which are exceptionally small. We also used this method and the Marcus formalism for nonadiabatic electron transfer to assess the electronic coupling matrix element.[12] Both approaches afforded nearly identical values: compare 2.3 cm^{-1} in THF to the values listed in Table S1. Most importantly, the electronic coupling in **4**, with values of 5.8 and 5.5 cm^{-1} in benzonitrile and THF, respectively, is unusually strong, considering that a distance of 40 Å separates the electron donor from the electron acceptor. In this light, the coupling of the *ex*TTF moiety to the oligo-PPVs, achieving full conjugation, is critical.

To analyze the charge-recombination mechanism, we probed the radical pair lifetimes between 272 and 350 K, which are summarized in Figure 2. The Arrhenius plots for the monomer, dimer (not shown), and trimer can be separated into two distinct sections: the low-temperature regime (i.e., <320 K) and the high-temperature regime (i.e., >320 K). The weak temperature dependence in the 272−320 K range suggests that a stepwise charge recombination via a transient **C$_{60}^{\bullet-}$−wire$^{\bullet+}$−*ex*TTF** can be ruled out, leaving electron tunneling via superexchange as the operative mode. This picture is in sound agreement with the thermodynamic barrier, necessary to overcome in forming **C$_{60}^{\bullet-}$−wire$^{\bullet+}$−*ex*TTF**. At higher temperatures (i.e., >320 K), the picture changes, and the strong temperature dependence suggests a thermally activated charge recombination. The activation barriers (E_a), derived from the slopes (**1**, 0.8 eV; **2**, 0.6 eV; **3**, 0.5 eV), confirm the HOMO (C_{60})−HOMO (wire) energy gap. Interestingly, the **C$_{60}^{\bullet-}$−wire−*ex*TTF**$^{\bullet+}$ pair in **4** reveals a contrasting trend with charge recombination that slows down substantially in the high-temperature region.

In principle, electron and hole transfer may both contribute to the charge recombination. Figure S3 shows that large LUMO (C_{60})−LUMO (wire) gaps of at least 1.1 eV result exclusively in an electron tunneling mechanism. Hole transfer from the HOMO at C_{60} to the HOMO at *ex*TTF, on the other hand, may proceed via superexchange or hopping. In fact, the temperature dependence helps to recognize the interplay between both processes. Once the hopping mechanism dominates, especially in **3** and **4**, and the hole migrates first to the wire, good HOMO (C_{60})−HOMO (wire) energy matching and strong electronic coupling lead to a kinetically fast and spectroscopically not resolvable recovery of the ground state.

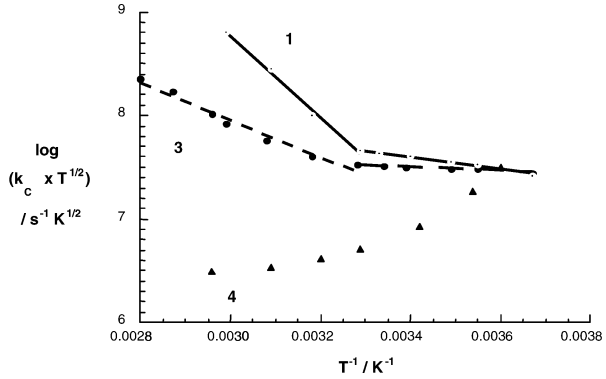

Figure 2. Arrhenius analyses of the temperature-dependent electron-transfer rate constants (k_{CR}) for **1**, **3**, and **4** in deoxygenated benzonitrile.

In summary, we demonstrated wire-like behavior in a series of **C$_{60}$−wire−*ex*TTF** over distances of 40 Å and beyond. Important for an exceptionally small attenuation factor (β) of 0.01 ± 0.005 Å^{-1} is that the energies of the C_{60}'s HOMOs match especially those of the long oligo-PPVs. This facilitates electron/hole injection into the wire. Equally important is the strong electronic coupling, realized through the paraconjugation of the oligo-PPVs into the *ex*TTF electron donor, which leads to donor−acceptor coupling constants (V) of ∼5.5 cm^{-1} and assists charge-transfer reactions that reveal a rather weak distance dependence.

Acknowledgment. This work has been supported by the MCyT of Spain (Project BQU2002-00855) and the Office of Basic Energy Sciences of the U.S. Department of Energy (NDRL-4520).

Supporting Information Available: Experimental details and supplementary figures and tables. This material is available free of charge via the Internet at http://pubs.acs.org.

References

(1) (a) *Molecular Electronics*; Jortner, J., Ratner, M., Eds.; Blackwell: Oxford, 1997. (b) *An Introduction to Molecular Electronics*; Petty, M. C., Bryce, M. R., Bloor, D., Eds.; Oxford University Press: New York, 1995. (c) Barbara, P. F.; Meyer, T. J.; Ratner, M. A. *J. Phys. Chem*. **1996**, *100*, 13148.
(2) For a recent review on molecular electronics, see: Carroll, R. L.; Gorman, C. B. *Angew. Chem., Int. Ed*. **2002**, *41*, 4378.
(3) (a) *Electronic Materials: The Oligomer Approach*; Müllen, K., Wegner, G., Eds.; Wiley-VCH: Weinheim, 1998. (b) Martin, R. E.; Diederich, F. *Angew. Chem., Int. Ed*. **1999**, 1350. (c) Tour, J. M. *Chem. Rev*. **1996**, *96*, 537.
(4) Hradsky, A.; Bildstein, B.; Schuler, N.; Schottenberger, H.; Jaitner, P.; Ongania, K.-H.; Wurst, K.; Launay, J.-P. *Organometallics* **1997**, *16*, 392.
(5) Davis, W. B.; Svec, W. A.; Ratner, M. A.; Wasielewski, M. R. *Nature* **1998**, *396*, 60.
(6) Pourtis, G.; Beljonne, D.; Cornil, J.; Ratner, M. A.; Brédas, J. L. *J. Am. Chem. Soc*. **2002**, *124*, 4436.
(7) Prato, M.; Maggini, M. *Acc. Chem. Res*. **1998**, *31*, 519.
(8) Martín, N.; Pérez, I.; Sánchez, L.; Seoane, C. *J. Org. Chem*. **1997**, *62*, 5690.
(9) Echegoyen, L.; Echegoyen, L. E. *Acc. Chem. Res.* **1998**, *31*, 593.
(10) (a) Heinze, J.; Mortensen, J.; Müllen, K.; Schenk, R. *J. Chem. Soc., Chem. Commun.* **1987**, 701. (b) Schenk, R.; Gregorius, H.; Meerholz, K.; Heinze, J.; Müllen, K. *J. Am. Chem. Soc*. **1991**, *113*, 2634.
(11) This rules out that the hole resides at the oligo-PPVs or is delocalized over the oligo-PPVs/*ex*TTF.
(12) Marcus, R. A. *Angew. Chem., Int. Ed. Engl.* **1993**, *32*, 1111.

JA0318333